Icarus 297 (2017) 240–251

Contents lists available at ScienceDirect

Icarus

journal homepage: www.elsevier.com/locate/icarus

The role of pre-impact topography in impact melt emplacement on terrestrial planets

C.D. Neish[a,b,*], R.R. Herrick[c], M. Zanetti[a,b], D. Smith[a]

[a] Department of Earth Sciences, The University of Western Ontario, London, ON N6A 5B7, Canada
[b] Centre for Planetary Science and Exploration, The University of Western Ontario, London, ON N6A 5B7, Canada
[c] The University of Alaska Fairbanks, Fairbanks, AK 99775, United States

ARTICLE INFO

Article history:
Received 7 March 2017
Revised 26 June 2017
Accepted 12 July 2017
Available online 13 July 2017

Keywords:
Impact processes
Cratering
Moon
Moon, surface
Venus

ABSTRACT

On terrestrial planets, flow-like deposits of impact melt are commonly found exterior to fresh impact craters. Often, these deposits are asymmetric about the crater rim, and the direction of flow may relate to either the pre-impact topography or the impact azimuth. In this work, we seek to determine the primary mechanism responsible for impact melt emplacement on two very different terrestrial worlds: the Moon and Venus. Newly derived stereo topography data allows us to investigate the role of pre-impact topography in melt emplacement on Venus for the first time. We determine that pre-impact topography plays an important role in melt emplacement around complex craters on the Moon but not on Venus. This difference may relate to the differences in gravity (and hence, crater depth and melt volume) on the two worlds. Melt trapped in the relatively deep lunar craters may require additional momentum to be pushed over the crater rim, and therefore emerges preferentially from the region of rim crest low. This added momentum might come from uplift during the crater modification stage. For the shallower craters on Venus, the downrange momentum imparted in oblique impacts may be sufficient to push the melt up and over the crater rim, explaining the correlation between melt direction and impact azimuth. Understanding the emplacement of impact melt on terrestrial planets of different sizes and geologic histories provides added insight into the impact cratering process.

1. Introduction

Flow-like deposits of impact melt are commonly observed on terrestrial planets, typically around young fresh craters (Shoemaker et al., 1968; Howard and Wilshire, 1975; Hawke and Head, 1977; Phillips et al., 1991; Prockter et al., 2010; Osinski et al., 2011; Tornabene et al., 2012). The melt is produced from the high shock pressures experienced during the impact event (Melosh, 1989, p. 46; Pierazzo et al., 1997; Osinski et al., 2013). During the excavation and modification stages of impact crater formation, melt can be ejected from the crater, where it can then flow under the influence of gravity. Knowledge of the emplacement history of the melt generated by impact provides a means to study the impact process itself.

Melt distribution patterns exterior to impact craters tend to be asymmetric, and their directionality may relate to either the pre-impact topography or the impact direction (Hawke and Head, 1977; Chadwick and Schaber, 1993; Osinski et al., 2011; Neish et al., 2014). On the Moon, most complex craters have melt directions that are coincident with the lowest point on the crater rim, implying that pre-existing topography plays a dominant role in melt emplacement on that world (Neish et al., 2014). This relationship may be the result of movement during the modification stage of crater formation, as the central uplift imparts an outward-directed flow to the melt, pushing it over a topographically low portion of the crater rim (Hawke and Head, 1977; Osinski et al., 2011).

On Venus, high-resolution topography data is scarce, so the effect of pre-impact topography has never been assessed for melt emplacement around its craters. Although the Magellan mission provided high-resolution views of the surface of Venus in the form of synthetic aperture radar (SAR) images at a resolution of ~100 m (Saunders et al., 1992), global altimetry was acquired at a significantly lower resolution (~10–20 km) (Ford and Pettengill, 1992). As a result, previous studies were only able to consider the importance of impact direction on impact melt emplacement on Venus. Chadwick and Schaber (1993) determined that ~92% of the melt flows associated with bilaterally symmetric ejecta patterns on Venus (indicative of a low impact angle) originated within 90° of

* Corresponding author at: Department of Earth Sciences, The University of Western Ontario, London, ON N6A 5B7, Canada.
E-mail address: cneish@uwo.ca (C.D. Neish).

http://dx.doi.org/10.1016/j.icarus.2017.07.004
0019-1035/

the downrange direction, suggesting a link between impact direction and melt emplacement. (For comparison, impact direction was determined for 31/55 melt-bearing complex craters on the Moon, and of these, only 55% had melt flows that originated within 90° of the downrange direction (Neish et al., 2014).) However, 35% of craters on Venus associated with radially symmetric ejecta (indicative of a high impact angle) were also observed to possess melt flows (Chadwick and Schaber, 1993). In these cases, it is unclear what factor determined the direction of melt emplacement.

Fortunately, it is possible to derive higher resolution topography data on Venus through the use of radar stereogrammetry, i.e., by comparing SAR images taken of the same area at different look angles. Previous work (Herrick and Rumpf, 2011) has generated topography for all craters on Venus with diameter $D > 15$ km that are located in the ~20% of the planet covered by same-side stereo. "Same-side" stereo refers to the situation where both images are collected with the SAR pointing in the same compass direction. In the case of Magellan, eastward-looking data was acquired during the first and third Venus days (or "Cycles") of science operation. Topography generated from the Magellan same-side stereo has a vertical resolution of ~50–100 m and a horizontal resolution of 1–2 km.

This new stereo-derived topography data set allows us to investigate the role of pre-impact topography in melt emplacement on Venus for the first time. We then compare the results to data previously published for impact craters on the Moon. In many respects, Venus and the Moon represent two important end members among the terrestrial planets. Venus is a geologically active body with abundant volcanism and tectonism shaping its surface; the Moon is a relatively inactive world shaped primarily by impact cratering. By determining the primary mechanism for impact melt emplacement on these two very different terrestrial worlds, we will better understand the impact cratering process in general.

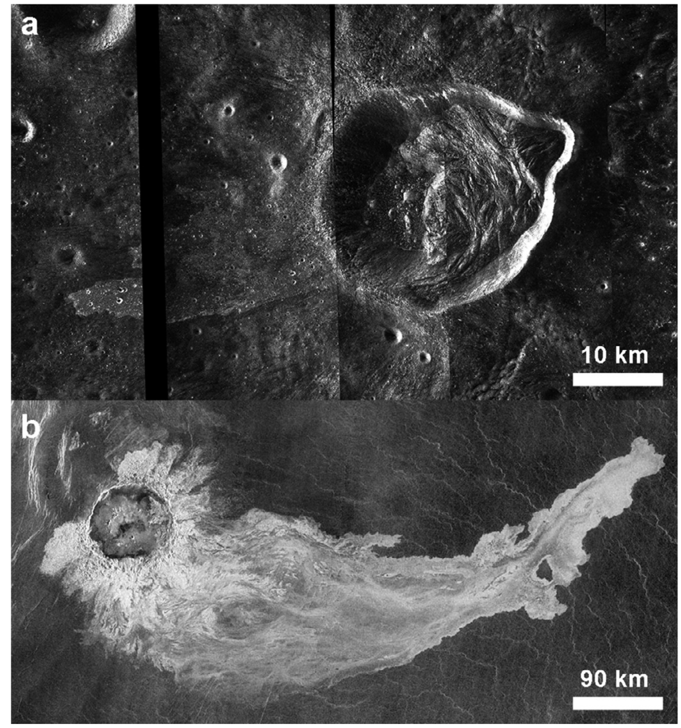

Fig. 1. S-Band (12.6 cm) synthetic aperture radar images of impact melt flows on (a) the Moon (observed to the west of Gerasimovich D crater) and (b) Venus (observed to the east of Addams crater). North is up in both cases.

2. Observations and methods

2.1. Moon

Lunar impact melts possess a variety of forms, including ponds, viscous flow features, and veneers (thin layers of melt that are draped over terrain, which then harden to form a relatively smooth upper rock layer) (e.g., Howard and Wilshire 1975; Hawke and Head, 1977; Bray et al., 2010; Denevi et al., 2012; Stopar et al., 2014). The volume of melt generated in an impact changes as a function of the impact crater diameter (Cintala and Grieve, 1998), as does the morphology of the melt deposits. Previous work suggested that hard-rock veneers are prominent in the smallest craters on the Moon ($D < 10$ km), while in larger craters, ponds and flows are the dominant melt morphology (Hawke and Head, 1977). More recent work (e.g., Carter et al., 2012; Stopar et al., 2014; Neish et al., 2014) suggests that flows can form even in these smaller craters, and the morphology of some impact melts imply movement after its initial emplacement (Bray et al., 2010; Denevi et al., 2012). Lunar impact melts appear very bright at radar wavelengths (with circular polarization ratios often in excess of one), suggesting a surface that is blocky at a scale of centimeters to decimeters, even though they appear quite smooth at the meter scale (Neish et al., 2017; Fig. 1a). These roughness properties are unlike any terrestrial lava flow yet studied, and may relate to differences in the surface texture of the melt caused by their unique emplacement and/or cooling environment.

Exterior deposits of impact melt have been reported for 146 craters on the Moon, ranging in diameter from 1.5 km to 316.4 km (Neish et al., 2014). We use a subset of this data set as input for this study. Specifically, we focus on central peak craters, to aid in comparison to craters on Venus, where simple craters are rare due to the disruption of small impactors in its thick atmosphere (Herrick et al., 1997; Korycansky and Zahnle, 2005). On the Moon, the transition between simple and complex craters occurs between a diameter of 10 and 20 km (Pike 1977). We selected 20 km as our minimum diameter, since craters with diameters between 10 and 20 km have transitional morphologies, with rim slumping but no obvious central peaks. To select our maximum diameter, we note that the onset diameter for peak-ring basins on the Moon is ~200 km, with protobasins appearing at a diameter of 137 km (Baker et al., 2011). Thus, we set an upper limit of $D = 100$ km for central peak craters in this study. This represents 49 impact craters from the original population of 146. The list of lunar craters examined in this work is given in Table 1. A large number of simple craters ($D < 5$ km) with exterior impact melt deposits were also identified in Stopar et al. (2014), but as the focus of this work is on complex craters, we will not consider this population further.

The majority of the craters studied in this work are morphologically fresh (classified as Copernican or Eratosthenian in age (Wilhelms, 1987)). As a result, they are not typically superposed by other impact craters, which could change their original rim elevations. Of these craters, only nine are found in the lunar mare. Indeed, there is a statistically significant lack of melt-bearing craters in the mare (Neish et al., 2014; Stopar et al., 2014), impeding any comprehensive comparisons between craters formed in the lunar basaltic plains to those formed in the Venusian basaltic plains.

We examined the topography of each crater of interest, using the 100 m/pixel Lunar Reconnaissance Orbiter (LRO) Wide Angle Camera (WAC) Stereo Digital Terrain Model (DTM) (Scholten et al., 2012). This data was overlaid on a WAC image of the crater of equal pixel scale. The depth of each crater was determined using two separate techniques, which we will refer to as d_1 and d_2 throughout the remainder of the manuscript. First, we determined depth d_1 using the methods outlined in Kalynn et al. (2013) for the Moon. Then, we determined depth d_2 using the technique outlined in Herrick and Sharpton (2000) for Venus. In this way, we could